$^{11}B+^{40}Ca$ single-nucleon transfer reactions $E_{lab}=51.5$ MeV

C. W. Glover, K. W. Kemper, and A. D. Frawley
Department of Physics, Florida State University, Tallahassee, Florida 32306
(Received 17 March 1980)

Angular distributions for the single-nucleon transfer reactions $^{40}Ca(^{11}B,^{12}C)^{39}K(J^\pi = 3/2^+$ and $1/2^+)$ and $^{40}Ca(^{11}B,^{10}B(J^\pi = 3^+$ and $1^+))^{41}Ca$ have been measured at 51.5 MeV. The distorted-wave Born approximation was used to analyze the data. The distorted waves used in the distorted-wave Born-approximation calculations were generated from both Woods-Saxon and double-folding optical potentials which describe elastic scattering data. The standard distorted-wave Born-approximation calculations reproduced the forward angle data, including the $l = 1$ pickup reaction, but overpredicted the back-angle data. Distorted-wave Born-approximation calculations carried out with distorted waves obtained from double-folded potentials were in much better agreement with the data. The extracted spectroscopic factors for the proton pickup reaction are much larger than those obtained from light-ion data while for the neutron stripping case they agree, even for the case where ^{10}B was in its first excited state.

[NUCLEAR REACTIONS $^{40}Ca(^{11}B,^{12}C)$, $^{40}Ca(^{11}B,^{10}B)$, $E=51.5$ MeV, measured $\sigma(\theta)$. DWBA analysis with Woods-Saxon and double-folding optical potentials.]

I. INTRODUCTION

It is hoped that heavy-ion transfer reactions may be used to obtain spectroscopic information complementary to that obtained from light-ion reactions. Before this can be accomplished, the transfer reaction mechanism must be understood. The angular distributions of heavy-ion induced, single-nucleon transfer reactions, measured at sufficiently high energies, display pronounced oscillations. In some cases, the phase, period of oscillation, and magnitude of the cross section are accounted for by exact finite range distorted-wave Born approximation calculations using Woods-Saxon optical model potentials determined from elastic scattering data to generate the distorted waves (conventional DWBA).

Several years ago, Bond *et al.*[1] pointed out the failure of conventional DWBA calculations to reproduce the results of $(^{13}C,^{14}N)$ proton pickup experiments on several calcium isotopes to well established $2s$-$1d$ shell model hole states in potassium. The results of the conventional DWBA gave the correct magnitude of the cross section but consistently oscillated out of phase with the data. The neutron stripping reaction $(^{13}C,^{12}C)$ did not exhibit this anomaly. A further study[2] involving the reactions $(^{14}N,^{15}O)$ and $(^{15}N,^{16}O)$ has shown no consistent pattern between the ability to describe the data and the physical reaction parameters.

To try to shed some light on the phasing problem, we measured angular distributions for $^{40}Ca(^{11}B,^{12}C)^{39}K(J^\pi = \frac{3}{2}^+$ and $\frac{1}{2}^+)$ and $^{40}Ca(^{11}B,^{10}B(J^\pi = 3^+$ and $1^+))^{41}Ca$ single nucleon transfer reactions at $E_{lab}=51.5$ MeV. These reactions were chosen to investigate whether the structure of the projectile-ejectile system is important in determining phasing of the angular distribution. The nucleon transfer for the ground state $(^{11}B,^{12}C)$ reaction occurs between $d_{3/2} \rightarrow p_{3/2}$ shell model orbits. For the reactions studied by Bond *et al.*[1,2] the transfer occurred from $d_{3/2} \rightarrow p_{1/2}$ shell orbits. For the $d_{3/2} \rightarrow p_{3/2}$ transition in the present work, there are more units of transferred angular momentum available for the $(^{11}B,^{12}C)$ reaction compared to the $(^{13}C,^{14}N)$ transition studied by Bond *et al.*[1] This allows better angular momentum matching between the entrance and exit channels thus reducing the importance of multistep processes. However, the angular distributions are not highly structured because of the range of transferred angular momenta. The $s_{1/2} \rightarrow p_{3/2}$ transition is oscillatory because only $l=1$ transfer is allowed, so that this transition provides a stringent test of our ability to describe the data. Woods-Saxon and double-folded optical potentials, determined from previously measured elastic scattering data, were used to generate the distorted waves in the exact finite range DWBA analyses carried out for the present reaction study.

II. EXPERIMENTAL METHOD

An inverted sputter[3] source was used to produce negative boron ions which were injected into the Florida State University super FN tandem Van de Graaff accelerator. The analyzed beam of 51.5 MeV $^{11}B^{+5}$ was directed into a multipurpose 46 cm diam scattering chamber to obtain data for angles $>10°$ (c.m.). Since oxygen contamination makes it difficult to extract the inelastic and elastic scattering yields at forward angles (i.e., $\theta_{c.m.} \leq 18°$)

needed for normalization purposes, the targets were made by evaporating about 125 $\mu g/cm^2$ of natural metallic calcium (96.8% ^{40}Ca) from a tantalum boat onto 15 $\mu g/cm^2$ carbon backings under vacuum, and then transferring the targets directly to the scattering chamber without breaking vacuum.

An array of two or three cooled silicon surface barrier counter telescopes consisting of 25 μm transmission counters (ΔE) and 100 μm stopping counters (E) were used to detect the reaction products. The E and ΔE signals were analyzed with conventional electronics and stored in an EMR 6130 on-line computer via a CAMAC interface between the ADC units and the computer. The raw events (ΔE vs E) were displayed on a two dimensional storage scope, gates were drawn around each particle type of interest, and the events were sorted by particle type into linear energy spectra ($E+\Delta E$).

To obtain small angle reaction data a 3-m quadrupole spectrometer (QS) was used.[4] The band pass, defined as the energy range of the reaction product for which the detection system has 100% efficiency, was measured to be approximately 1 MeV. A collimated E-ΔE counter telescope was placed at the focal position of the spectrometer. The events were stored and sorted by the computer in the same manner as described previously.

The quadrupole spectrometer was also used to obtain the small angle ^{10}B reaction data. Separation of the ^{10}B reaction products from the very intense elastically scattered ^{11}B group required time-of-flight (TOF) information, and this was obtained from a channel-plate detector located 2.7 m "upstream" from the E-ΔE telescope. A time resolution of 450 ps was obtained. The TOF, ΔE, and E signals were input to the computer where they were displayed on a two dimensional storage scope as [TOF vs $(E+\Delta E)$] and [ΔE vs E]. Gates were drawn around the ^{10}B particle group in each two dimensional display, and those events which were common to both gated regions were sorted into a linear energy spectrum. This provided very clean ^{10}B spectra. The QS data were normalized to the scattering chamber data by comparing yields at several overlap angles. A monitor detector was used throughout all measurements to check both the consistency of the charge integration and for any target deterioration. All relative cross sections are corrected for dead time and detector efficiency. To obtain the absolute cross sections for the scattering chamber data, the product of the target thickness and solid angle were determined by normalizing the elastic scattering data to that measured in Ref. 5. The combination of the 6% uncertainty quoted in Ref. 5 and the reproducibility of the normalization runs yields an uncertainty of 12% in the absolute cross section for this study.

III. ANALYSIS

The single proton pickup reactions $^{40}Ca(^{11}B,^{12}C)^{39}K(J^\pi=\frac{3}{2}^+$ and $J^\pi=\frac{1}{2}^+)$ and the single neutron stripping reactions $^{40}Ca(^{11}B,\ ^{10}B(J^\pi=3^+$ and $1^+))^{41}Ca$ were analyzed by assuming the reactions to be describable by the distorted-wave Born approximation (DWBA). The DWBA calculations were performed by the exact finite range computer code MERCURY.[6] The bound state wave functions of the transferred particle for both projectile and target were calculated using the energy separation procedure with a real Woods-Saxon (WS) potential having a radius $R=1.25A_{\text{core}}^{1/3}$ fm and diffuseness $a=0.65$ fm. In addition, an attractive spin-orbit parameter between the transferred particle and core of $\lambda=25$ was assumed. The spectroscopic factors for the transferred particle bound to the $1p$ shell nuclei involved were taken from Cohen and Kurath.[7] It was noticed here and by others[8] that small changes in the bound state form factors can change the magnitude of the DWBA cross section by as much as 50%, but they have little influence upon the shape of the cross section. Thus, the bound state wave functions described above were used for all calculations.

The distorted waves necessary for the analysis were generated from Woods-Saxon optical model potentials that describe previously measured[5] elastic scattering of the entrance and exit channel reaction products. It is assumed that these optical potentials define the nucleus-nucleus interaction potential over the region in R space where the transfer reaction takes place. The results of the DWBA calculations using the Woods-Saxon optical potentials in Table I to generate the distorted waves are shown as dashed curves in Figs. 1 and 2. The DWBA calculations predict the basic overall shape of the measured angular distributions. For the $l=1$ transfer reaction $^{40}Ca(^{11}B,^{12}C)^{39}K^*(J^\pi=\frac{1}{2}^+)$ the DWBA accurately reproduces the period and amplitude of the forward-angle oscillations, but the calculated cross section does not fall off as rapidly as the measured cross section. The same is true but to a lesser degree for the $^{40}Ca(^{11}B,^{10}B)^{41}Ca$ and $^{40}Ca(^{11}B,^{12}C)^{39}K(\frac{3}{2}^+)$ reactions. The spectroscopic factors extracted from these calculations are listed in Table II along with the corresponding light-ion spectroscopic factors. As can be seen, the heavy-ion results are much larger than the light-ion results for the proton pickup, but are in good agreement for neutron stripping even for the case where ^{10}B was detected

TABLE I. Optical model parameters for the reaction channels studied.

$$V = V_0(1 - e^{x_R})^{-1} + W_0(1 - e^{x_I})^{-1}$$

$$x_j = (r - R_j)/a_j \quad J = R, I$$

$$R_j = r_{0j} A_{\mathrm{TARG}}^{1/3}$$

System	Set		(MeV) V_0	(fm) r_{0R}	(fm) a_R	(MeV) W_I	(fm) r_{0I}	(fm) a_I
$^{11}B + ^{40}Ca$	A	WS	16.66	2.06	0.65	16.22	2.0	0.65
	B	DF-WS-EQ[a] (± 2)	49.33	1.92	0.6	10.0	2.14	0.65
$^{10}B + ^{40}Ca$	C	WS	24.5	2.02	0.65	21.5	2.02	0.65
	D	DF-WS-EQ(± 2)	61.0	1.91	0.596	35.0	1.87	0.63
	E	DF-WS-EQ(± 4)	226.9	1.65	0.626	30.5	1.88	0.68
$^{12}C + ^{39}K$	F	WS	57.9	1.97	0.605	41.4	1.92	0.623
	G	DF-WS-EQ(± 2)	55.4	1.94	0.594	42.8	2.03	0.455
	H	DF-WS-EQ(± 4)	185.44	1.73	0.62	42.77	1.88	0.606

[a]DF-WS-EQ denotes a Woods-Saxon potential well fit to the double-folding potential well ± 2 or ± 4 fm about the strong absorption radius.

in its first excited state. Thus, we conclude for these reactions that the conventional DWBA (i.e., one in which the elastic scattering WS optical potentials are used as the distorting potentials) is in good agreement with the shape of the data, with the exception that it underpredicts the rate of fall-off of the (^{11}B,^{12}C) reactions.

As was shown in Ref. 8, the magnitude of the (^{11}B,^{12}C) cross section is very sensitive to the bound state radius of the $p + ^{39}K$ system, while the shape is not. To reproduce the light-ion spectroscopic factors for the proton pickup reaction, the bound state radius for $p + ^{39}K$ had to be increased from $1.25(39)^{1/3}$ to $1.6(39)^{1/3}$. No such magnitude difficulty was encountered in Ref. 2.

The fact that the conventional DWBA overestimates the reaction strength at larger angles has been observed in many other single-nucleon trans-

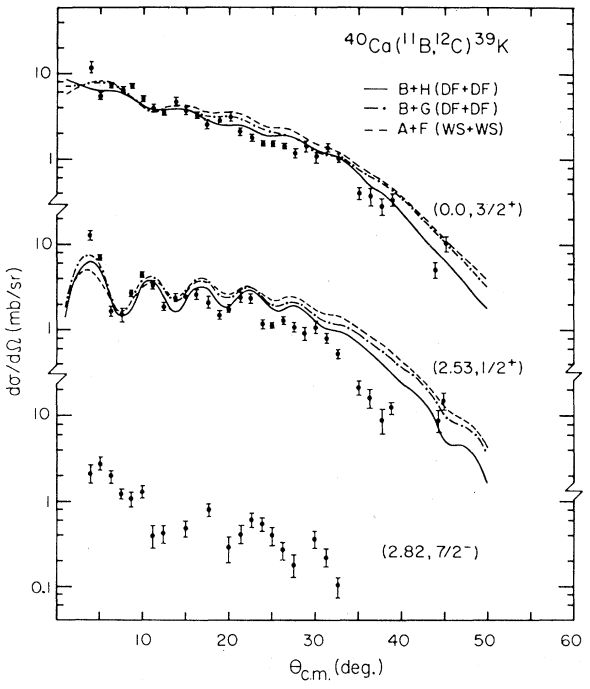

FIG. 1. The angular distributions for the single-proton pickup reactions, $^{40}Ca(^{11}B, ^{12}C)^{39}K$ ($J^\pi = \frac{3}{2}^+$ and $\frac{1}{2}^+$). The solid and – · – curves represent the DWBA calculations using entrance and exit distorted waves derived from the double-folding optical potential. The dashed curve is the DWBA calculation in which the distorted waves were derived from a Woods-Saxon optical potential. Also shown is the $^{40}Ca(^{11}B, ^{12}C)^{39}K(J^\pi = \frac{7}{2}^-)$ angular distribution.

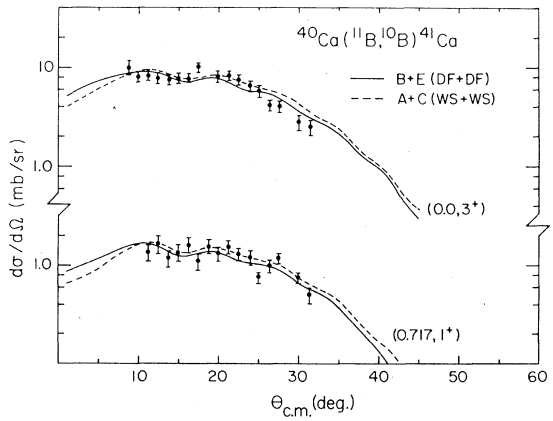

FIG. 2. The angular distributions for the single neutron stripping reactions $^{40}Ca(^{11}B, ^{10}B\,(J^\pi = 3^+$ and $1^+))^{41}Ca$. The solid curve represents the DWBA calculations using distorted waves derived from the double-folding optical model. The dashed curve is the DWBA calculations using distorted waves generated from the Woods-Saxon optical potential.

TABLE II. Spectroscopic factors obtained from the relationship $\sigma_{exp}=C^2S_1C^2S_2\sigma_{MERC}$. The value of C^2S_1 was obtained from Cohen and Kurath, Ref. 7.

Reaction	Final state	Q (MeV)	C^2S_2 [a]	C^2S_2 [b,c]
$^{40}Ca(^{11}B,^{12}C)^{39}K$	$(0.0,\frac{3}{2}^+)$	7.623	9.5	4.85
^{39}K	$(2.53\ \text{MeV},\frac{1}{2}^+)$	5.093	4.8	1.05
$^{40}Ca(^{11}B,^{10}B\ \text{g.s.})^{41}Ca$ g.s.		−3.093	0.83	0.8
$^{40}Ca(^{11}B,^{10}B_1)^{41}Ca$ g.s.		−3.810	0.64	

[a] Represents an average spectroscopic factor derived by averaging all spectroscopic factors obtained from each DWBA calculation with different optical model parameter sets.
[b] From Cossairt *et al.*, Phys. Rev. C 18, 23 (1978).
[c] From Seth *et al.*, Phys. Lett. 53B, 17 (1974).

fer reactions[9–11] in this mass region. The most general procedure to remedy this defect has been to arbitrarily increase the diffuseness (a_r) or radius of the real part of the WS potential for the exit channel. This procedure focuses the trajectories that skim the nuclear surface to more forward angles. The resulting optical potential then fails to reproduce the observed elastic scattering data.

More recent attempts to resolve this difficulty have included taking into account the effects of the inelastic target excitations coupling back into the elastic channel[12] and consideration of the state dependence of the exit channel distorting potential which arises because the energy levels of the transferred nucleon shift as a function of the separation of the colliding ions.[13] This latter process can be viewed as the creation of a particle-hole pair with respect to the entrance channel, which changes the Q value of the reaction and hence the distorted waves in the exit channel. An additional possibility is that the Woods-Saxon potential form used in the DWBA calculations does not correctly describe the nucleus-nucleus interaction in the region where the reaction takes place.

Recent studies[5,14] of double-folded (DF) potentials have shown that elastic scattering data can be described by potentials which have shapes different from the generally used WS form. It is possible that the adjustments in the exit channel parameters mentioned above merely compensate for incorrectly shaped distorting potentials.

To investigate the influence of double-folded potentials on transfer cross sections, the measured elastic scattering data $^{10,11}B+^{40}Ca$ and $^{12}C+^{39}K$ were reanalyzed using the DF optical model.[5] Because our DWBA code only allows WS shaped potentials, the resulting nucleus-nucleus interaction was then fitted to an "equivalent" WS potential in the region (±2 fm) around the strong absorption radius. Then these "equivalent" WS potentials were used to generate the distorted waves in the DWBA code MERCURY. The resulting angular distributions are shown as the dot-dashed curve in Fig. 1 and the solid curve in Fig. 2. From these figures, one sees that slight improvements in the DWBA cross sections occur when compared with conventional DWBA cross sections. Because of these suggestive improvements, a WS potential was fit to the DF potential over a range of ±4 fm around the strong absorption radius. It was not possible to find a WS equivalent potential for $^{11}B+^{40}Ca$ for the ±4 fm range that also fit the elastic scattering data. The DWBA calculations that make use of these equivalent potentials are represented by the solid curves in Fig. 1. No change was found for the $(^{11}B,^{10}B)$ reaction when the ±4 fm Woods-Saxon equivalent potentials were used compared to those for ±2 fm and the results are again given by the solid curve in Fig. 2. As can be seen, the use of DF potentials in the DWBA calculations reduces the proton pickup cross sections at larger angles, suggesting that these reactions sample a larger range of the nucleus-nucleus potential than does elastic scattering. This difference in potential range sampled by elastic scattering and reactions has been commented on earlier.[15] When the Woods-Saxon, double-folding and Woods-Saxon equivalent potentials are plotted in R space (see Fig. 3), the range over which these potentials differ is easily seen. From Fig. 3 it is seen that the Woods-Saxon and Woods-Saxon equivalent potentials differ significantly inside about 7 fm. All the potentials for each system have approximately the same value about the strong absorption radius (denoted by an arrow in Fig. 3). The fact that fitting the Woods-Saxon equivalent potentials over ±4 fm changed the shape of the transfer angular distribution indicates that the reaction is sensitive to

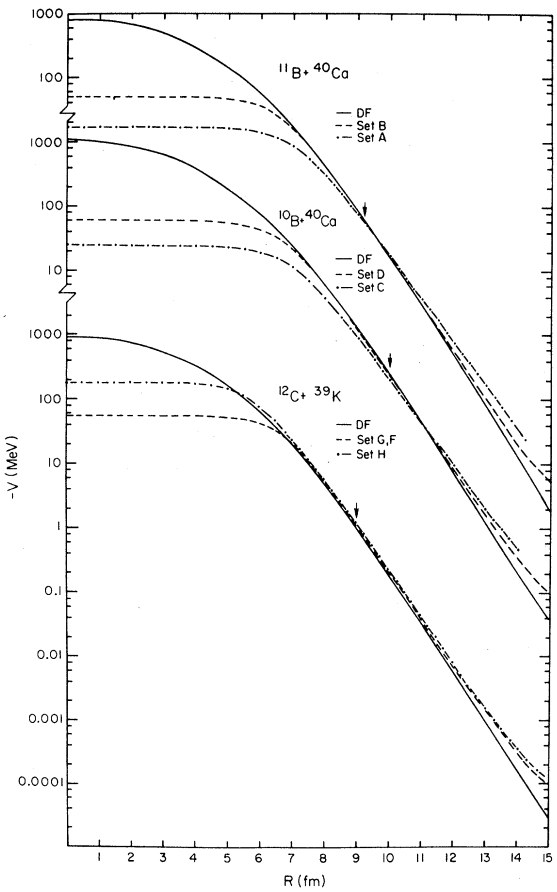

FIG. 3. The radial dependence of the real nuclear potential is shown for the potential sets of Table I. These potential sets were derived from elastic scattering data by using the double-folding (solid curve) and the Woods-Saxon optical potentials. For the $^{12}C+^{39}K$ system, potential sets *G* and *F* are represented by the same curve.

separation distances that are 3 fm smaller than the strong absorption radii.

Figure 2 contains data for the proton pickup reaction to the $\frac{7}{2}^-$ 2.82 MeV state in ^{39}K. Calculations were not carried out for this transition because this state is predominantly a single particle state rather than a hole state, implying that the population of this state occurs through multistep processes rather than a direct one step process as assumed here for the other transitions.

IV. CONCLUSION

In the present work proton pickup and neutron stripping for $^{11}B+^{40}Ca$ was studied. The single neutron transfer reactions are well described by the DWBA even when the ejectile is in an excited state. The proton pickup reaction to the ^{39}K $\frac{3}{2}^+$ ground state is also well described in shape by the DWBA calculations over quite an extensive angular range. For the $\frac{1}{2}^+$, 2.53 MeV ^{39}K, $l=1$ transition, the calculations are nicely in phase with the data. However, the rate of falloff with increasing angle is greater for the data than for the calculations. The use of double-folded potentials in the DWBA calculation improves the agreement with the data, implying that the transfer reaction is more sensitive to the interior of the interaction potentials than is elastic scattering. The magnitude of the extracted spectroscopic factors are in good agreement with light-ion results for the neutron transfer reaction, but are much larger for the proton transfer reaction. An increase in the proton bound state radius of about 25% is necessary to bring the light- and heavy-ion spectroscopic factors into agreement for the (^{11}B, ^{12}C) reaction.

In summary, the present work shows the need to obtain a better understanding of the shape of the nucleus-nucleus potentials involved in reactions before the role of multistep and dynamic energy level shifts can properly be assessed.

ACKNOWLEDGMENTS

The authors would like to thank Dr. Charles Maguire for extremely helpful discussions. This work was supported in part by the National Science Foundation.

[1]P. D. Bond, C. Chasman, J. D. Garrett, C. K. Gelbke, Ole Hansen, M. J. LeVine, A. Z. Schwarzschild, and C. E. Thorn, Phys. Rev. Lett. 36, 300 (1976).
[2]P. D. Bond, M. J. LeVine, D. J. Pisano, C. E. Thorn, and L. L. Lee, Jr., Phys. Rev. C 19, 2160 (1979).
[3]R. I. Cutler, K. W. Kemper and K. R. Chapman, Nucl. Instrum. Methods 164, 605 (1979).
[4]G. R. Morgan, G. D. Gunn, M. B. Greenfield, N. R. Fletcher, J. D. Fox, D. L. McShan and L. Wright, Nucl. Instrum. Methods 123, 439 (1975).
[5]C. W. Glover, K. W. Kemper, L. A. Parks, F. Petrovich, and D. P. Stanley, Nucl. Phys. A 337, 520 (1980).
[6]L. A. Charlton, Phys. Rev. C8, 146 (1973); L. A. Charlton and D. Robson, Florida State University Technical Report No. 5 (unpublished).
[7]S. Cohen and D. Kurath, Nucl. Phys. A101, 1 (1967).
[8]J. J. Bevelacqua, D. Stanley and D. Robson, Phys. Rev. C 15, 447 (1977).
[9]H. J. Korner, G. C. Morrison, L. R. Greenwood and R. H. Siemssen, Phys. Rev. C 7, 107 (1973).
[10]W. Henning, Y. Eisen, J. R. Erskine, D. G. Kovar, and B. Zeidman, Phys. Rev. C 15, 292 (1977); G. L. Bomar, C. F. Maguire, J. L. C. Ford, J. Gomez del Campo and D. Shapira, Bull. Am. Phys. Soc. 24, 842 (1979).
[11]D. G. Kovar, W. Henning, B. Zeidman, Y. Eisen,

J. R. Erskine, H. T. Fortune, T. R. Ophel, P. Sperr and S. E. Vigedor, Phys. Rev. C 17, 83 (1978).
[12]K. S. Low, T. Tamura, and T. Udagawa, Phys. Lett. 67B, 5 (1977).
[13]E. A. Seglie, J. F. Petersen and R. J. Ascuitto, Phys. Rev. Lett. 42, 956 (1979).
[14]G. R. Satchler and W. G. Love, Phys. Rep. 55, 183 (1979).
[15]A. J. Baltz, P. D. Bond, J. D. Garrett, and S. Kahana, Phys. Rev. C 12, 136 (1975).